Pressure dependence of Superconductivity in Amorphous Ni_xZr_{100-x} Alloys

by

Fariba Mahini Abyaneh

A Thesis

submitted to the Department of Physics

in partial fulfilment of the requirements

for the degree of

Master of Science

July 1988

Brock University

St. Catharines, Ontario

ACKNOWLEDGMENTS

I would like to express my sincere appreciation to Dr. F. S. Razavi for suggesting, supervising and helping in the long and tedious process of completing this thesis and Dr. Z. Altounian for preparing the samples and performing x-ray measurements on $Ni_{20}Zr_{80}$.

I also wish to thank Dr. Mitrovic for his helpful advice. It is a pleasure to thank the technical staff of Brock university machine shop, electronic shop and the glass blower.

Lastly the support and encouragement of my family and friends is greatly appreciated.

ABSTRACT

Pressure variations of the superconducting transition temperature T_c of a series of amorphous Ni_xZr_{100-x} alloys have been studied under quasihydrostatic pressures upto 8 G Pa. For amorphous samples having Ni-concentration less than 40%, $\partial T_c/\partial P$ is positive in sign and it decreases non linearly with increase in x, whereas $\partial T_c/\partial P$ is negative in sign for Ni concentration of 45%.

Comparison with the Hall coefficient [1] and the thermoelectric power [2] results for the same amorphous alloys leads to the conclusion that s-d hybridization nature of the d-band (Ni) plays a central role in the sign reversal behaviour. Application of pressures greater than 2 G Pa to $Ni_{20}Zr_{80}$ led to the formation of a new phase, ω-Zr , which retains its form after the pressure is released.

TABLE OF CONTENTS

LIST OF TABLES

LIST OF ILLUSTRATIONS

Chapter 1

INTRODUCTION

Crystals do not provide an appropriate medium for the systematic variation of physical parameters. Systematic variations in physical parameters such as the electron phonon interaction, the Debye temperature and spin fluctuations are best achieved by varying the concentration of an existing element in the alloy. This presents difficulties in dealing with crystals because the alloys considered do not have a solid solution across the composition range. Mixed phases or changes in crystal structures create different phonon structures and electron density of states thus making it hard to segregate the effect of the physical parameter under consideration. At this point metallic glasses are used because they do not have a particular crystal structure. Their physical parameters change smoothly over a composition range, easily allowing the study of electrical or magnetic properties.

The first amorphous superconductor was discovered by Buckle and Hilsch [3] in 1954. Amorphous Bismuth was prepared by vapour deposition onto cryogenic substrates. This work was followed by an extensive study of the superconducting properties of amorphous

substances. Later on, other methods of preparation of amorphous substances were also employed, namely sputtering [4], chemical deposition [4], electrodeposition [4] and rapid quenching from the liquid state [5]. The latter is considered as one of the most widely used methods of obtaining amorphous metals commonly known as metallic glasses. At room temperature these metals stay in an amorphous state for long periods of time.

In 1973, the first systematic study on the superconducting properties of amorphous alloys of transition elements was carried out by Collver and Hammond[6]. They measured the superconducting transition temperature (T_c) of alloys of 4d and 5d transition elements. They found that T_c varies as a function of electron to atom ratio. In these studies amorphous metals were in the form of thin films. In 1975, Johnson et al [7] reported the first series of amorphous Lanthanum Gold transition metal superconductors obtained by liquid quenching. Later, other amorphous transition metals were obtained by that technique. These alloys usually consist of an early transition metal such as Zr or Nb and a late transition metal such as Ni or Fe. Rapp et al [8] obtained T_c of amorphous $Ni_{30}Zr_{70}$ to be about 3 K. That result was followed by work of Babic et al[9] who

measured T_c and magnetic susceptibilities of amorphous Ni_xZr_{100-x} and found that T_c decreases linearly with the increase in x.

Zr has a partially filled 4-d band and can form eutectic mixtures with almost all 3-d transition elements in a wide range of concentration. Their alloys will produce various types of materials from ferromagnetic to superconducting metallic glasses. We have chosen to study the system Ni_xZr_{100-x} because it provides a wide range of amorphous alloys (where x=20 to 45).

Ni_xZr_{100-x} amorphous alloys are superconducting at low temperatures [10] (for x=20 to 45, T_c=3.97 to 1.83 K) and T_c decreases with increase in Ni concentration. Batalla et al [11] have calculated λ_{sf} of Ni_xZr_{100-x} amorphous alloys using the modified McMillan equation for transition temperature which includes the electron spin mass enhancement factor λ_{sf}. They found the value of λ_{sf} to be $.01<\lambda_{sf}<0.12$ for $0.20=<x=<0.64$. The other properties, such as the Hall coefficient and the thermoelectric power have been studied by Cochrane et al [1] and Altounian et al [2] respectively. They have observed experimentally that

the Hall coefficient and the thermopower are strong functions of composition and change their sign at the Ni rich end. They concluded that the position and width of the 3-d component of the density of states at the fermi level plays a central role in the cross over behaviour.

The purpose of this work is to study the possible effect of spin fluctuation on the superconductivity of amorphous Ni_xZr_{100-x} using the high pressure technique. Spin fluctuation effects are expected to be sharply reduced by pressure in almost all cases on the basis of either localized or band models [12]. We attempt to determine how the high pressure affects T_c and from that find out whether spin fluctuation effects are pronounced in these particular alloys.

In chapter 2, the theory of superconductivity and the effect of spin fluctuations in determining the value of the transition temperature is discussed. Also the structure, preparation and properties of amorphous alloys are explained. Chapter 3 deals with the experimental procedures. Data and calculations are presented in chapter 4. Chapter 5 contains the discussion and Chapter 6 the conclusion.

Chapter 2

THEORY

2.1-Theory of superconductivity

In the normal state the resistivity of metals and alloys is generally temperature dependent. However the resistivity of some metals and alloys suddenly drops to zero at low temperatures. The temperature at which the transition occurs is known as the superconducting transition temperature (T_c). This phenomenon was first observed by Kamerlingh Onnes [13] when he was measuring the resistance of mercury at liquid helium temperature.

The superconducting state also exhibits very dramatic magnetic properties. A bulk superconductor will act like a perfect diamagnet in the presence of weak magnetic fields. When the specimen is cooled below the transition temperature and placed in low magnetic fields, the magnetic flux does not enter the specimen. The superconductor will also exhibit the ejection of magnetic flux present in the specimen after it is cooled through the transition temperature (low magnetic fields). This is known as the Meissner effect. If the applied magnetic field is sufficiently strong the superconductivity can be destroyed. This critical value of the magnetic

field is known as the critical magnetic field $H_c(T)$. At T_c, $H_c(T) = 0$ [14]. Detailed reviews of the properties of superconductivity are available in most solid state texts such as Introduction to Solid State Physics[14].

The superconducting state is an ordered state of the conduction electrons of the metal. The order is in the formation of loosely bound pairs of electrons known as Cooper pairs[14].

Cooper[15] first calculated the binding energy of two electrons in the presence of a non interacting electron gas

$$E = -2\hbar w_d \exp\left(-\frac{2}{N(0)V}\right)$$

where w_d is phonon frequency, $N(0)$ is the electronic density of states at the Fermi level, and V is the pairing potential arising from electron phonon interaction.

Later, Bardeen, Cooper and Schrieffer [15] laid down the basis for the quantum theory of superconductivity and suggested that the transition temperature could be estimated from the following equation

$$T_c = 1.14 \frac{\hbar \omega_D}{k_B} \exp\left(-\frac{1}{N(0)V}\right)$$

where k_B is the Boltzman constant.

The BCS theory was able to predict T_c for some simple metals but failed to do so for transition elements and compounds.

In 1968 McMillan[16] applied the strong coupling theory of superconductivity to transition metal superconductors . He predicted the following equation to determine approximately the superconducting transition temperature as a function of electron-phonon and electron-electron coupling constants .

$$T_c = \frac{\theta_D}{1.45} \exp\left[-\frac{1.045(1+\lambda)}{\lambda - \mu^*(1+0.62\lambda)}\right]$$

where θ_D is the Debye temperature, λ is the electron phonon coupling constant and μ^* is the Coulomb pseudo potential.

Using the above formula for calculating T_c of d band elements and compounds, somehow overestimates T_c . This may indicate a fault in the scheme of calculation or it may be taken as a sign that the repulsive interaction is larger than the ordinary estimate of μ^* ($0.1 < \mu^* < 0.13$). This discrepancy is believed to be caused by the presence of spin fluctuations or paramagnons[17] .

The repulsive interaction among the opposite spin electrons keeps them apart which indicates an attraction between an electron and an

opposite spin hole, as the electron-electron interaction increases, the electron-hole excitation stays together longer and longer in both space and time. At the ferromagnetic instability the pair is fully bound. Before one reaches the instability the system can locally fluctuate into the particle-hole bound state. These fluctuations have many effects on the properties of the system. The nature of spin fluctuations in weak ferromagnetic and antiferromagnetic metals is different than in a local moment system. The magnetic order in the case of local moments is destroyed by thermal excitations of spin flips. They are described as the correlated motion of well-defined local moments, whereas in the weak ferromagnetic metals, the magnetic order is destroyed by the thermal excitations of the long wavelength spin fluctuation and it can not be explained in terms of well defined local moments (because the local amplitude of spin fluctuations varies with temperature) [18].

Garland and Benneman [12] have suggested that the influence of spin fluctuations may be included in a modified McMillan equation as

$$T_c = \frac{\langle \omega^2 \rangle^{1/2}}{1.2} \exp\left\{ -\frac{1 + \lambda + \lambda_{sf}}{0.96\lambda - (1 + 0.6\lambda)(\mu^* + \lambda_{sf})} \right\} \quad ---(1)$$

where λ_{sf} is the spin fluctuation mass enhancement factor and $\langle w^2 \rangle$ is the average squared phonon frequency.

Generally, the transition temperature of the elements that are considered to have spin fluctuations is expected to increase when applying pressure. An analysis of the modified McMillan equation for the transition temperature reveals that this variation is caused by the volume dependence of either the Debye temperature θ_D ($\theta_D \simeq [\langle w^2 \rangle]^{1/2}\hbar/K_B$), the electron phonon coupling constant λ, the spin fluctuation mass enhancement factor λ_{sf} or the Coulomb pseudo potential μ^*. The volume dependence of $\theta_D(v)$ is described by the Gruneisen parameter γ_G.

$$\gamma_G(\theta) = -\partial \ln \theta_D / \partial \ln V$$

Detailed reviews of the theory of superconductivity, the effect of pressure on T_c and spin fluctuation can be found in Superconductivity in d and f band metals [12], Solid State Physics [14] and Spin Fluctuations in Itinerent Electron Magnetism [18].

2.2-Amorphous material

To analyse the formation of solids, isolated atoms must be considered which are brought closer until an interatomic distance of solids

results. An experiment relating to this would be to cool down the vapours of some material until liquid is obtained and further cooling the material until it solidifies. The volume versus temperature results are given by Zallen [5] and plotted in Fig(2-1). The two sharp breaks in curve (1) denote the phase change from gas to liquid at the boiling temperature, T_b, and further cooling, the phase change from liquid to solid at T_m.

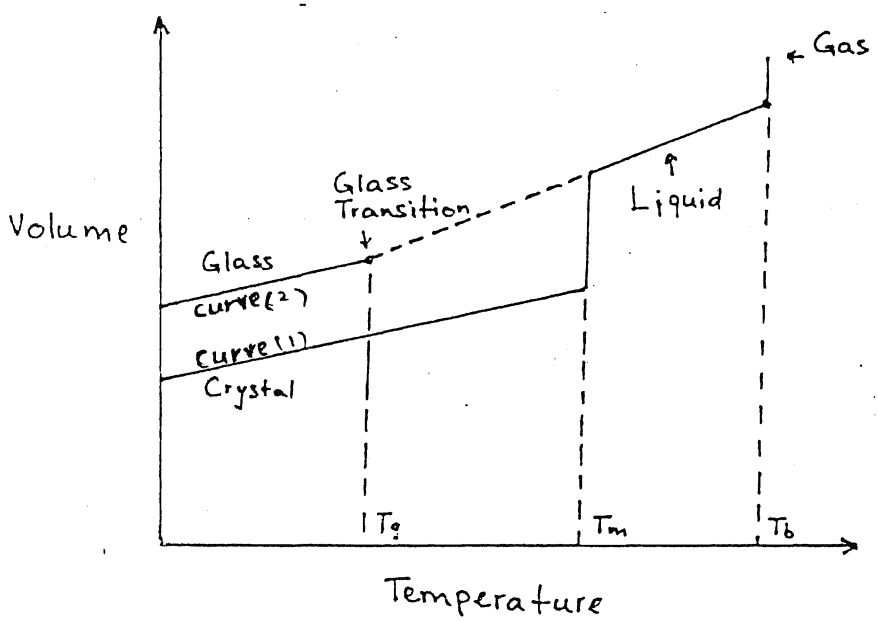

Fig(2-1)

General behaviour of volume with temperature

However, if the liquid is subjected to very high cooling rates rather than following curve (1) it would have followed along curve (2) solidifying into the amorphous form. The temperature at which the amorphous material is formed is called the glass forming temperature, T_g. (At a temperature slightly larger than T_g the metalic glass recrystalizes.)

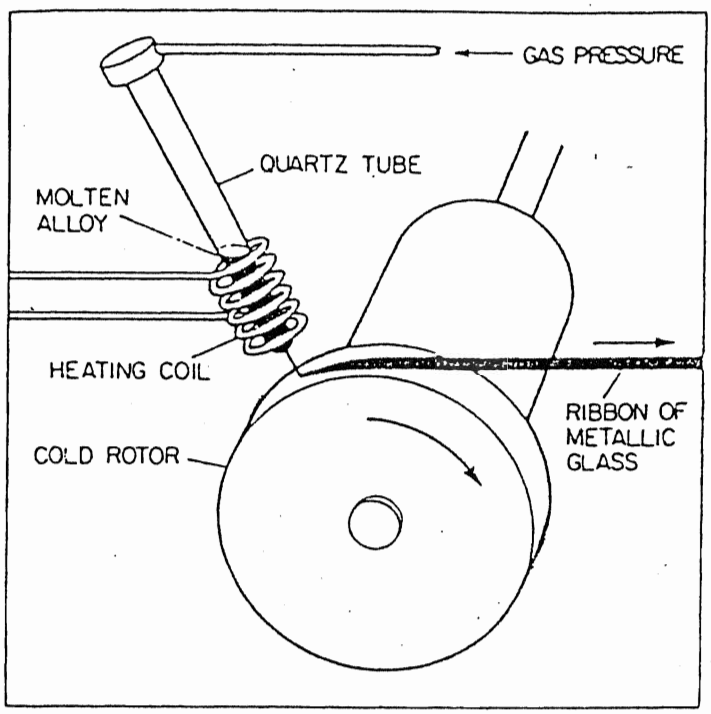

Fig(2-2)

Melt spinning of metalic glass (After Zallen , Richard (5)).

There are several ways of preparing amorphous materials. The most common method is the melt spinning technique according to Zallen [5]. With this method, a molten alloy is extruded through an orifice by means of gas pressure to form a molten jet. It is, then, impinged upon a cool and rotating substrate to form a glassy material (figure(2-2)).

The structure of metallic glasses has been studied with the aid of different scattering experiments, namely X-ray, neutron and electron scattering experiments ; where a monochromatic beam is scattered by the sample and the intensity of the scattered beam is measured as a function of the scattering angle. The intensity is proportional to the structure factor. The scattering angle determines the scattering vector. A graph of the structure factor versus the scattering vector will show typical forms for crystal, liquid and the gas[19].

The arrangement of atoms is described in terms of a pair correlation or radial distribution function (RFD) which determines the probability of finding two ions separated by the distance r. RFD is essentially the Fourier transform of the structure factor.

The structure factor versus scattering vector shows Bragg peaks for crystals (Fig(2-3)), damped oscillatory peaks for liquids (Fig(2-4)) and a constant for gases (Fig(2-5)). The neutron scattering data for an

Figure (2-3)

Radial distribution function of solids

Figure (2-4)

Radial distribution function of liquids

Figure (2-5)

Radial distribution function of gases

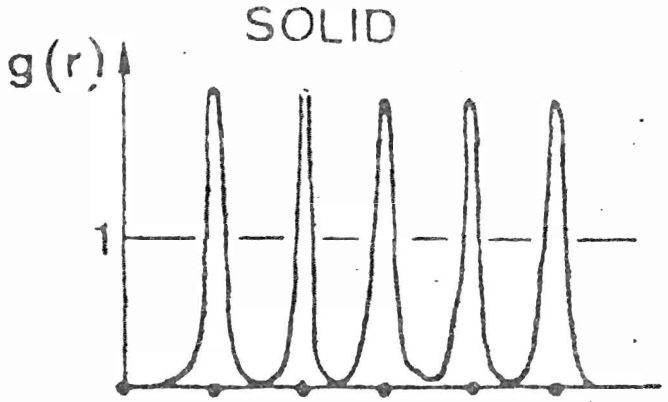
SOLID
g(r)
1

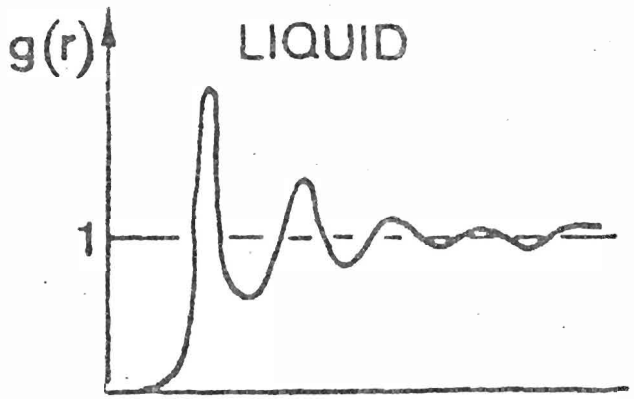
g(r)
LIQUID
1

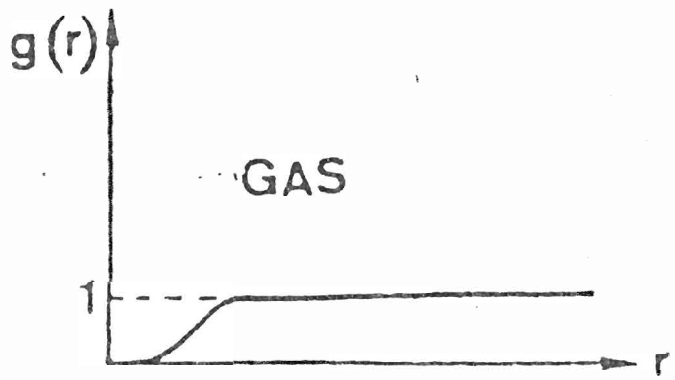
g(r)
GAS
1
r

Figure (2-6)

Neutron scattering intensity versus scattering vector of amorphous material

(After Guntherodth, H. J. (19))

Figure (2-7)

Schematic sketches of the atomic arrangements in

a) crystal,

b) amorphous solid,

c) gas.

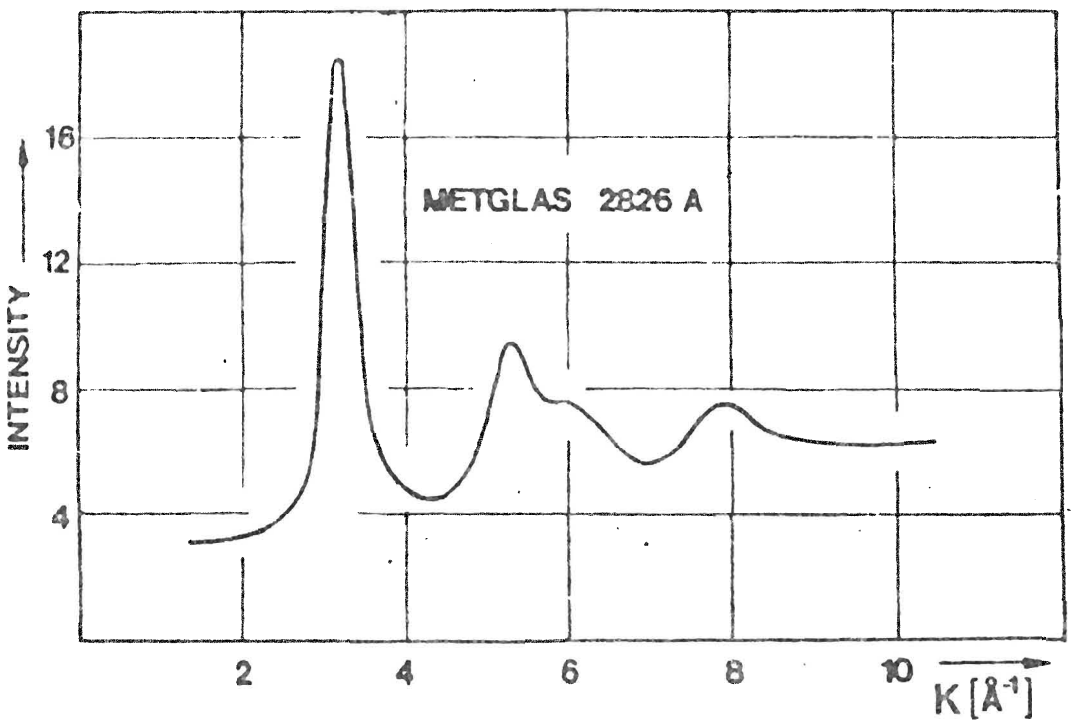
METGLAS 2826 A
INTENSITY
16
12
8
4
2
4
6
8
10
K [Å⁻¹]

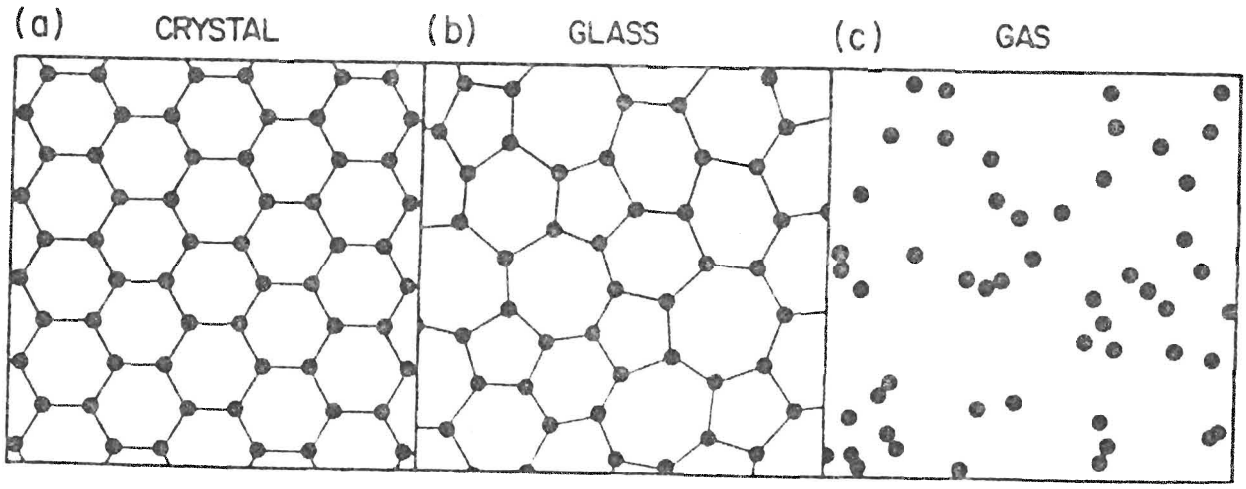
(a) CRYSTAL
(b) GLASS
(c) GAS

amorphous sample is sketched in fig(2-6). The pattern is very much like that of a liquid with the only difference in the second maximum which shows two peaks for amorphous materials. The difference in the structure of an amorphous material and crystal is the absence of long range order (as can be seen from neutron scattering experiment).

Figure (2-7) a, b and c represents schematic characteristics of atomic arrangements in crystals, glasses and gases[5].

We can see that the atomic arrangements in amorphous material are not random but they have a high degree of local correlation, whereas in gases the atoms are randomly distributed. The short range order in amorphous materials is a consequence of the chemical bonding responsible for holding the solid together.

2.3-NiZr amorphous alloy

The phase diagram of NiZr is shown in the figure(2-8) [20]. Amorphous alloys can be prepared for various compositions between 20 to 90 atomic percent of Ni. The range from 40 to 60 atomic percent of Ni was called the forbidden range but recently alloys have been prepared over this range [20].

Figure (2-8)

Phase diagram of Ni-Zr

(After Altounian et al. (20))

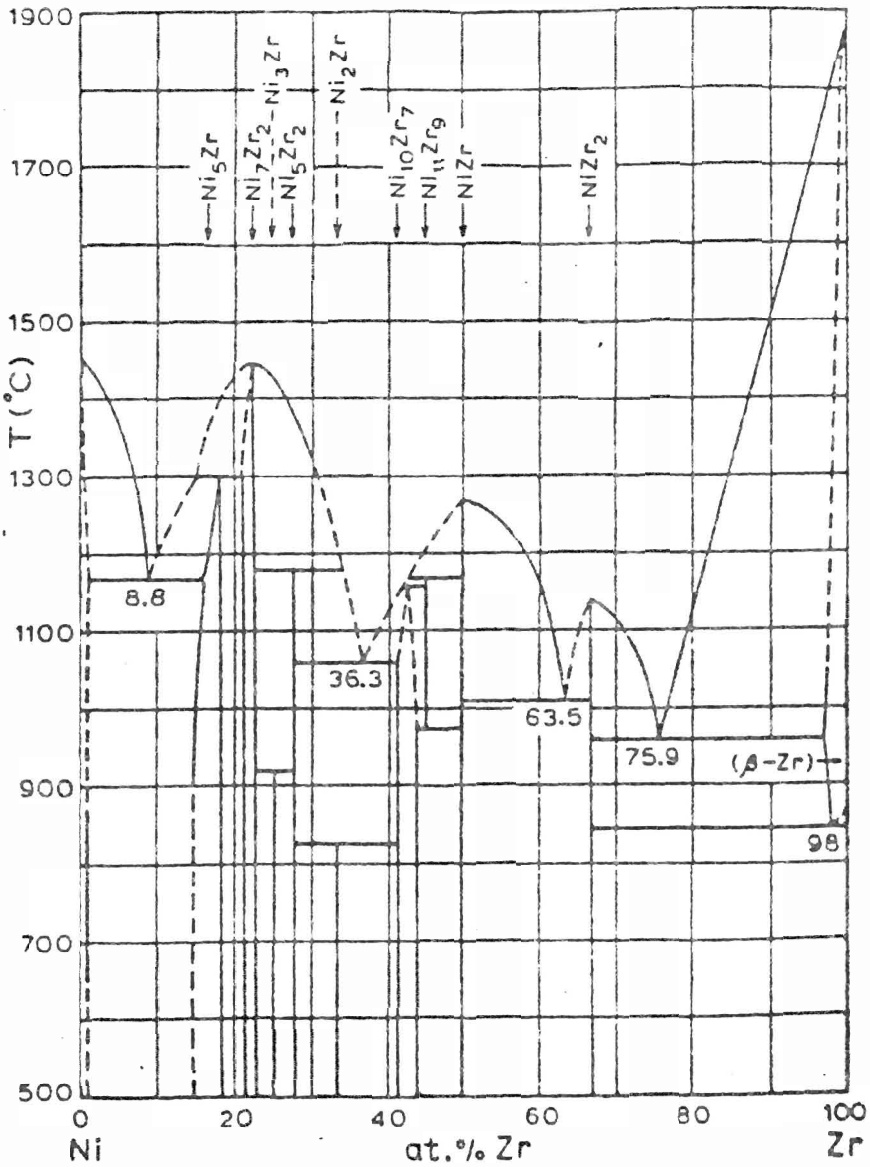
1900
1700
1500
1300
1100
900
700
500
T (°C)
0
20
40
60
80
100
Ni
at.% Zr
Zr
Ni5Zr
Ni7Zr2
Ni3Zr
Ni5Zr2
Ni2Zr
Ni10Zr7
Ni11Zr9
NiZr
NiZr2
8.8
36.3
63.5
75.9
(β-Zr)
98

Buschow et al [21] studied the thermal behaviour of the alloy using Differential Scanning Calorimetry (DSC). The room temperature magnetic susceptibilities of these alloys were analysed by Batalla et al.[11].

Chapter 3

METHODS

3.1- Samples

The experiment was performed on amorphous $Ni_x Zr_{100-x}$ where x varies from 20 to 45. Samples were prepared by Dr. Z. Altounian of the Department of Physics, McGill University using melt spinning.

Amorphous ribbons were prepared by melt spinning buttons of approximately 1.5 grams of crystalline material. The buttons were made by arc melting appropriate amount of Zr (99.99% pure) with Ni (99.999% pure) under Titanium-gettered Argon atmosphere. Each button was melted several times to ensure homogeneity. The melt spinning took place under Helium at 50 k pa pressure on the rim of a copper wheel that had a tangential velocity of about 50 ms^{-1}. Debye Scherrer X ray photographs of these amorphous ribbons showed no sharp lines after 24 hours exposure. The ribbons were typically 20-30 μm thick and 1.5 mm wide.

The samples were stored at room temperature since they remain stable up to around 500 K.

3.2-Pressure cell

The pressure dependence of the superconducting transition temperature (T_c) of each amorphous alloy was measured under quasihydrostatic pressure up to 8 G Pa.

The quasihydrostatic pressure cell consists of a pyrophyllite gasket with steatite disks used as the pressure transmitting medium. A piece of lead is used as a pressure manometer. The overall construction of the high pressure device is shown in figure (3-1).

Pressure is applied to the cell by two opposing Carbon Tungsten anvils which are mounted on Copper Beryllium support rings. The clamp (1) is pressure loaded using a Carver laboratory press, the force acting on the cell is frozen by tightening a screw (2).

The sample is placed between two steatite disks, figure (3-2). Six electrical leads were laid down on six grooves, cut in the pyrophyllite ring. This allows a high accuracy four point electrical resistivity measurements on the amorphous sample as well as a lead sample.

The superconducting transition temperature of lead decreases with the increase in pressure. The values of T_c versus pressure for lead given by Eichler and Witting [22] are plotted in figure (3-3) and were used to

Figure (3-1)

Schematic diagram of the pressure cell.

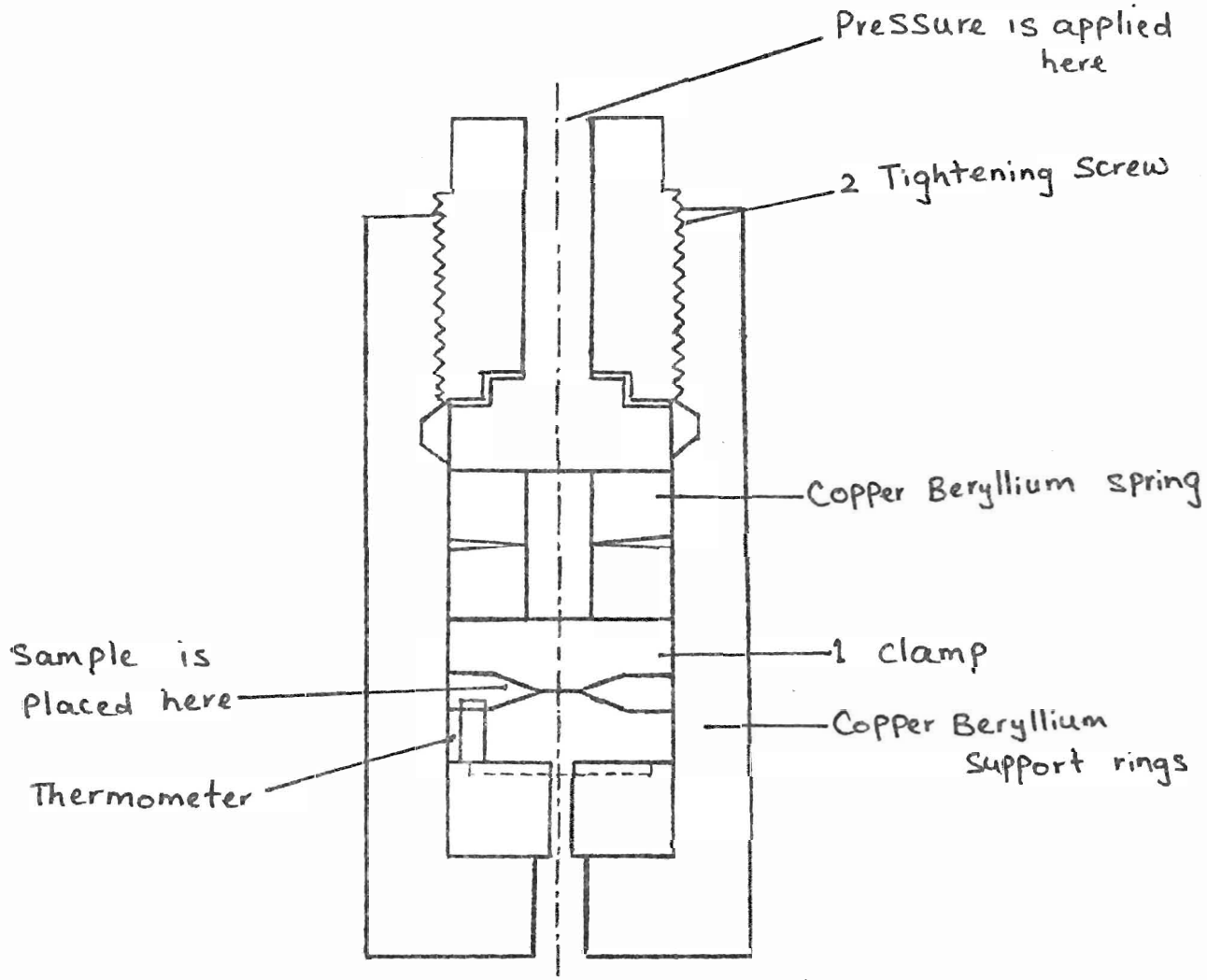
Pressure is applied here
2 Tightening Screw
Copper Beryllium spring
1 clamp
Copper Beryllium Support rings
Sample is placed here
Thermometer

Figure (3-2)

Schematic diagram of sample holder

Quasihydrostatic Pressure

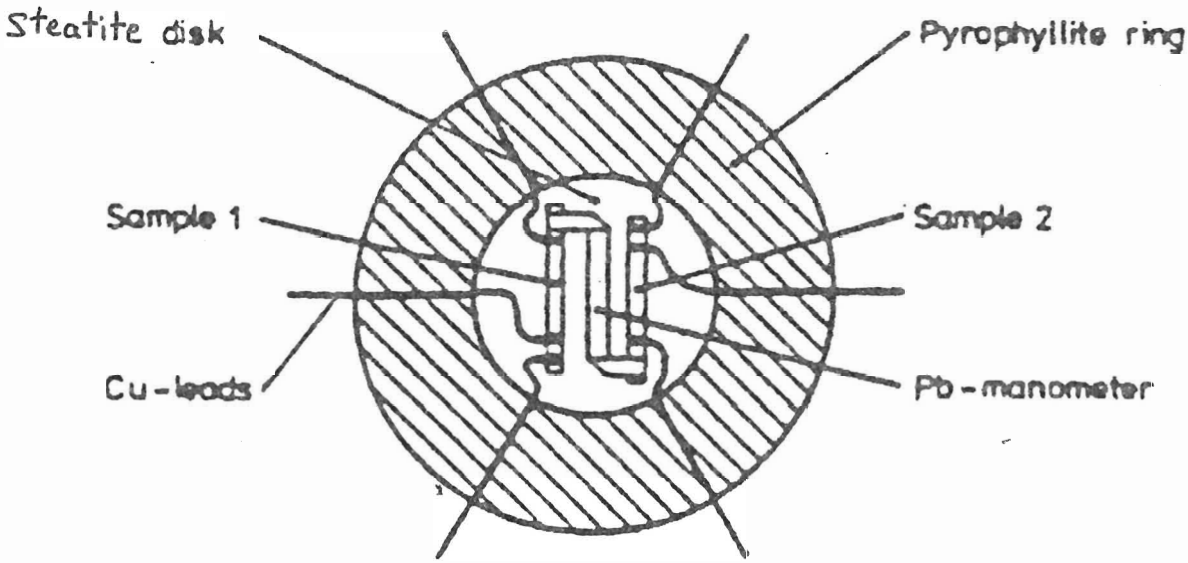

a)

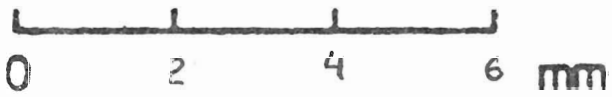

Figure (3-3)

Graph of transition temperature of Lead versus pressure.

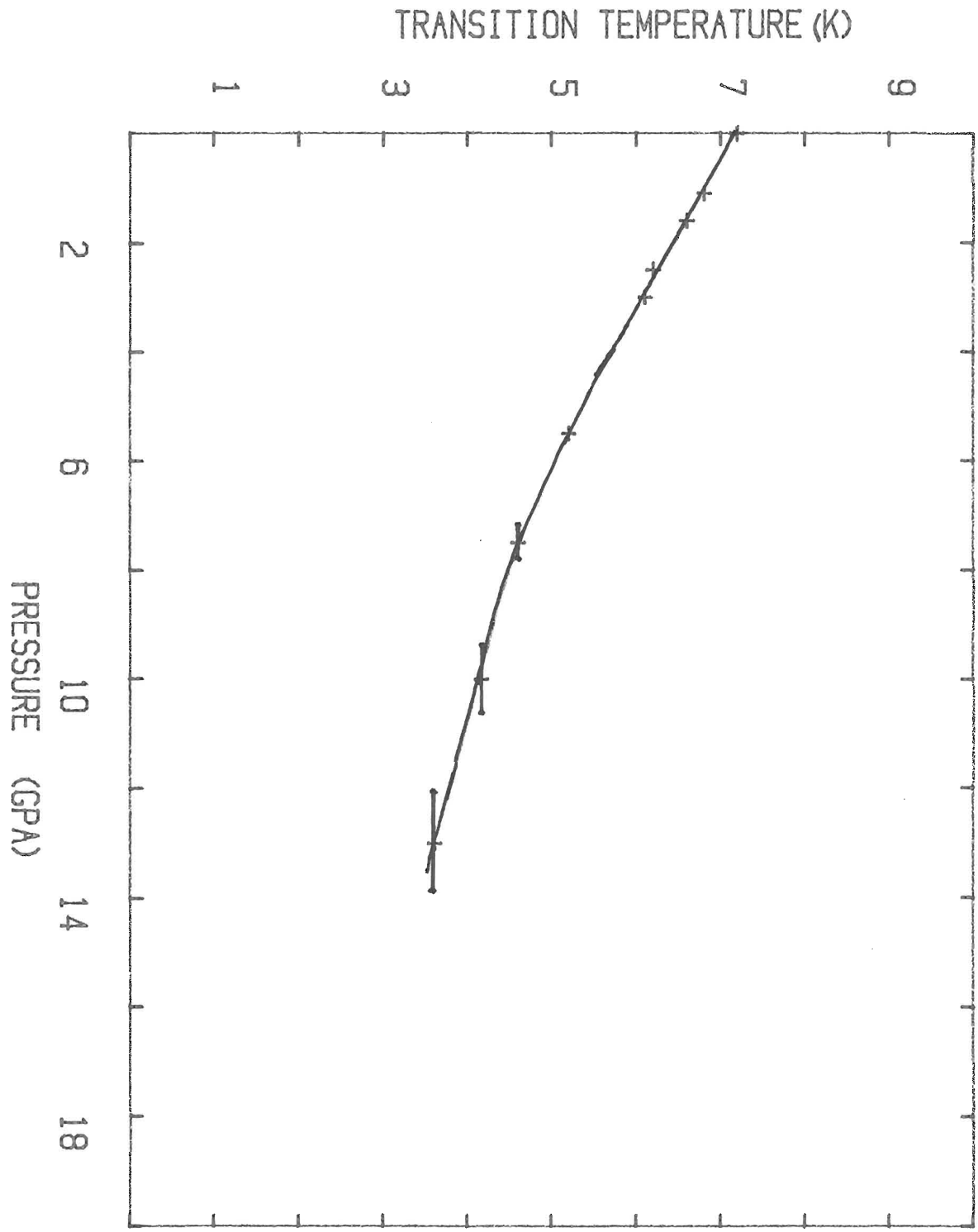
TRANSITION TEMPERATURE (K)
1
3
5
7
9
PRESSURE (GPA)
2
6
10
14
18

determine the pressure. Temperature is measured using a calibrated carbon glass thermometer which is kept as close to the sample as possible to minimize the temperature gradient. The pressure cell is kept in an inner dewar, which in turn is placed in the outer dewar. The sample is initially cooled by transferring liquid nitrogen into the outer dewar to about 90 K. Then it is cooled to 4.2 K by transferring liquid Helium into the inner dewar. The temperature is further reduced to 1.4 K by pumping on the liquid Helium in the inner dewar.

The schematic diagram of the apparatus used to measure the resistivity of lead as well as the amorphous sample is shown in figure(3-4). A current of 2 to10 mA is passed through the sample and the lead, the voltage across the amorphous alloy is measured with a Keithley 181 NanoVoltmeter, the voltage across the lead is monitored by a Keithley 150 A Microvolt Ammeter. The thermometer is supplied with a current of 100 micro Amperes. The voltage across it, is measured with a NLS (Non Linear Systems) Digital voltmeter X-1. The entire system is connected to a computer so that at chosen intervals the computer reads the value of the voltages. The resistivities and the temperatures are then, calculated and these data are saved on a disk.

Figure (3-4)

Schematic diagram of the resistivity measuring device.

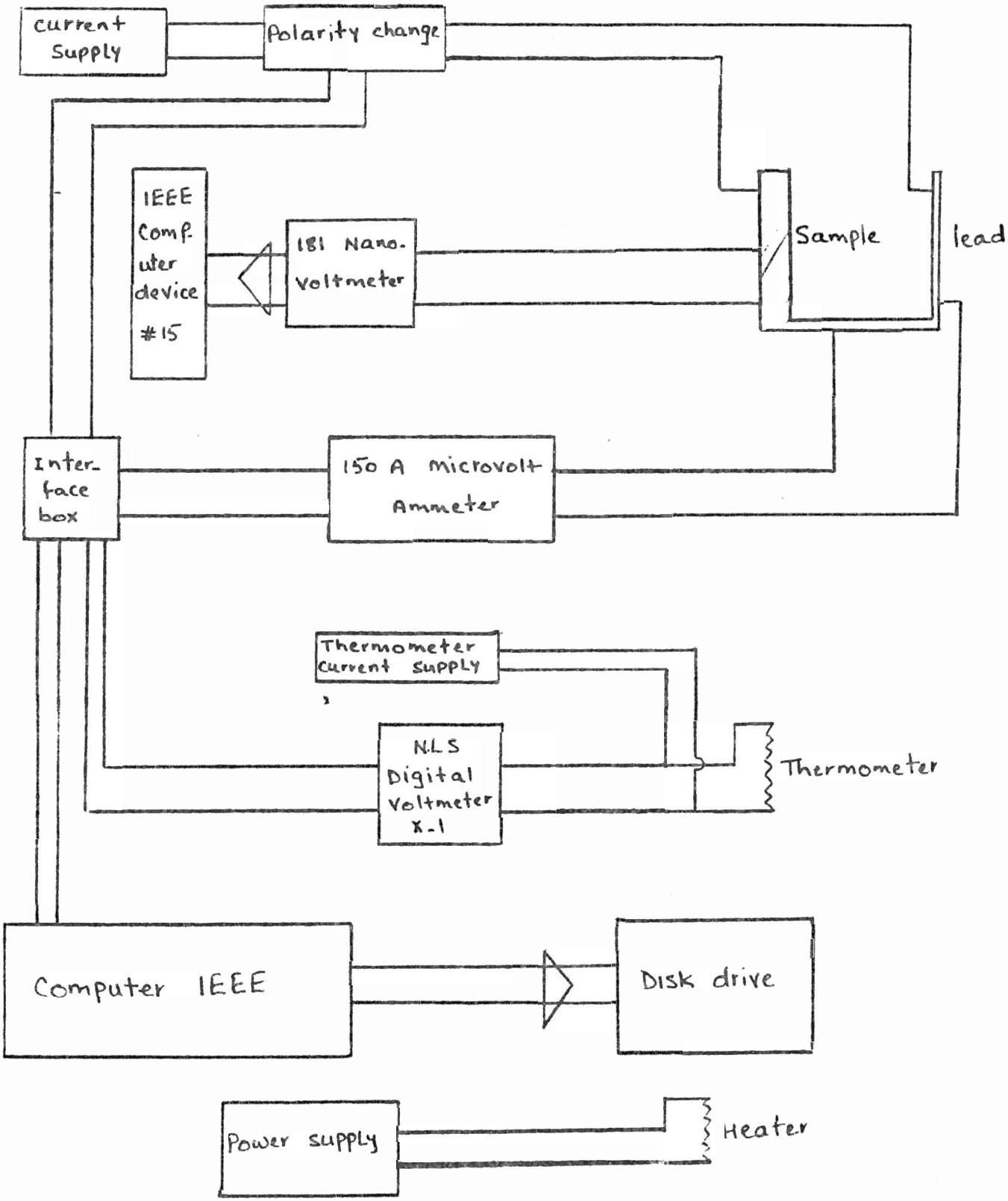
current Supply
Polarity change
IEEE Comp. uter device #15
181 Nano. Voltmeter
Sample
lead
Inter- face box
150 A microvolt Ammeter
Thermometer current supply
N.L.S Digital Voltmeter X-1
Thermometer
Computer IEEE
Disk drive
Power supply
Heater

At each measurement we change the direction of the current in order to eliminate the thermoelectric voltage induced at the wire contacts. A heater is wound around the cell in order to enable us to raise the temperature at an appropriate rate.

Chapter 4

RESULTS

The resistivity of Ni_xZr_{100-x} with x =20, 29, 36.5 , 40, 45 was measured in a temperature range of 300 K down to 1.5 K at pressures up to about 8 G Pa.

The pressure is monitored by the superconducting transition temperature of lead as obtained by resistivity measurements. The resistivity of lead is constantly measured when the cell is warming up. A typical graph showing normalised resistivity of Pb versus the temperature at the pressure of 3.5 G Pa is plotted in figure (4-1). At various pressures the resistivity of the lead as a function of temperature remains essentially the same (with the exception of a shift in the superconducting transition temperature to lower temperature for higher pressures).

The amorphous materials have small and negative temperature coefficient of resistivity which arise from their high degree of disorder. The plot of resistivity versus temperature for Ni_xZr_{100-x} remains almost a straight line almost to the superconducting transition temperature where

Figure (4-1)

Graph of resistivity of Lead versus temperature at a pressure of 3.5 GPa.

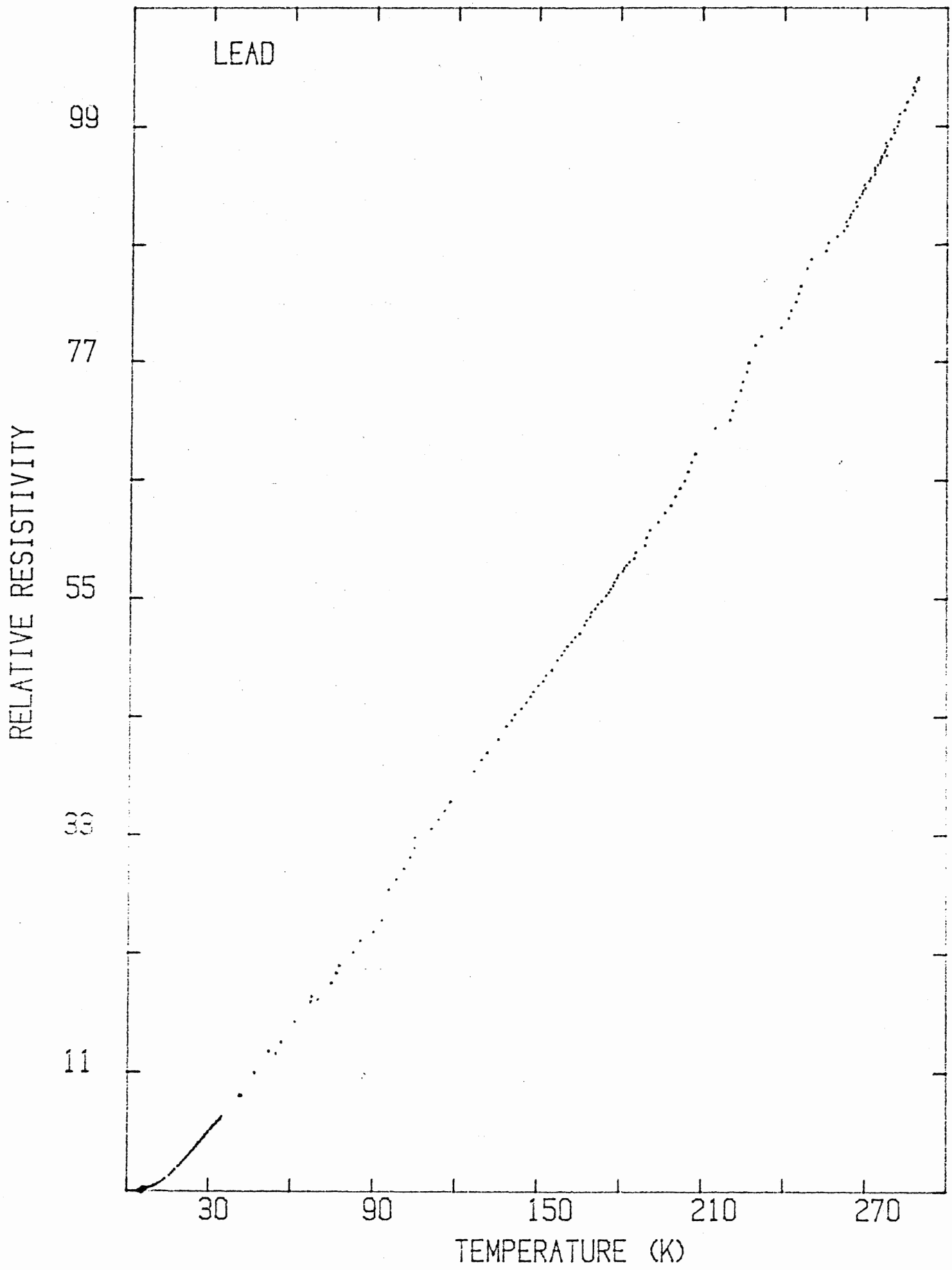
LEAD
99
77
55
33
11
RELATIVE RESISTIVITY
30
90
150
210
270
TEMPERATURE (K)

there is a sharp transition to zero resistivity. The temperature width is of the order of 0.1 K. One such example is shown in figure (4-2) for $Ni_{40}Zr_{60}$.

Figure (4-3) shows a graph of resistivity versus temperature at low temperature for $Ni_{20}Zr_{80}$ at pressures 1.8, 3.0, 4.2, 5.4, 7.0 and 7.9 G Pa. From the graph it can be seen that with increase in pressure the transition temperature, as well as the transition temperature width, increases. At pressures higher than 1.8 G Pa two transitions have been observed. This behavior could be attributed to the fact that $Ni_{20}Zr_{80}$ is at the limit of the glass forming edge, with the possibility of formation of minute fractions of crystal and/or the presence of two phases of amorphous material at high pressure.

Figures (4-4) to (4-9) show the rate of change in transition temperature with pressure for all the alloys. Table 1 exhibits the percentage concentrations of the Ni in the alloy and the superconducting transition temperature at zero pressure obtained from extrapolating graphs (4-4) to (4-9).

Figure (4-2)

Graph of resistivity of $Ni_{40}zr_{60}$ versus temperature.

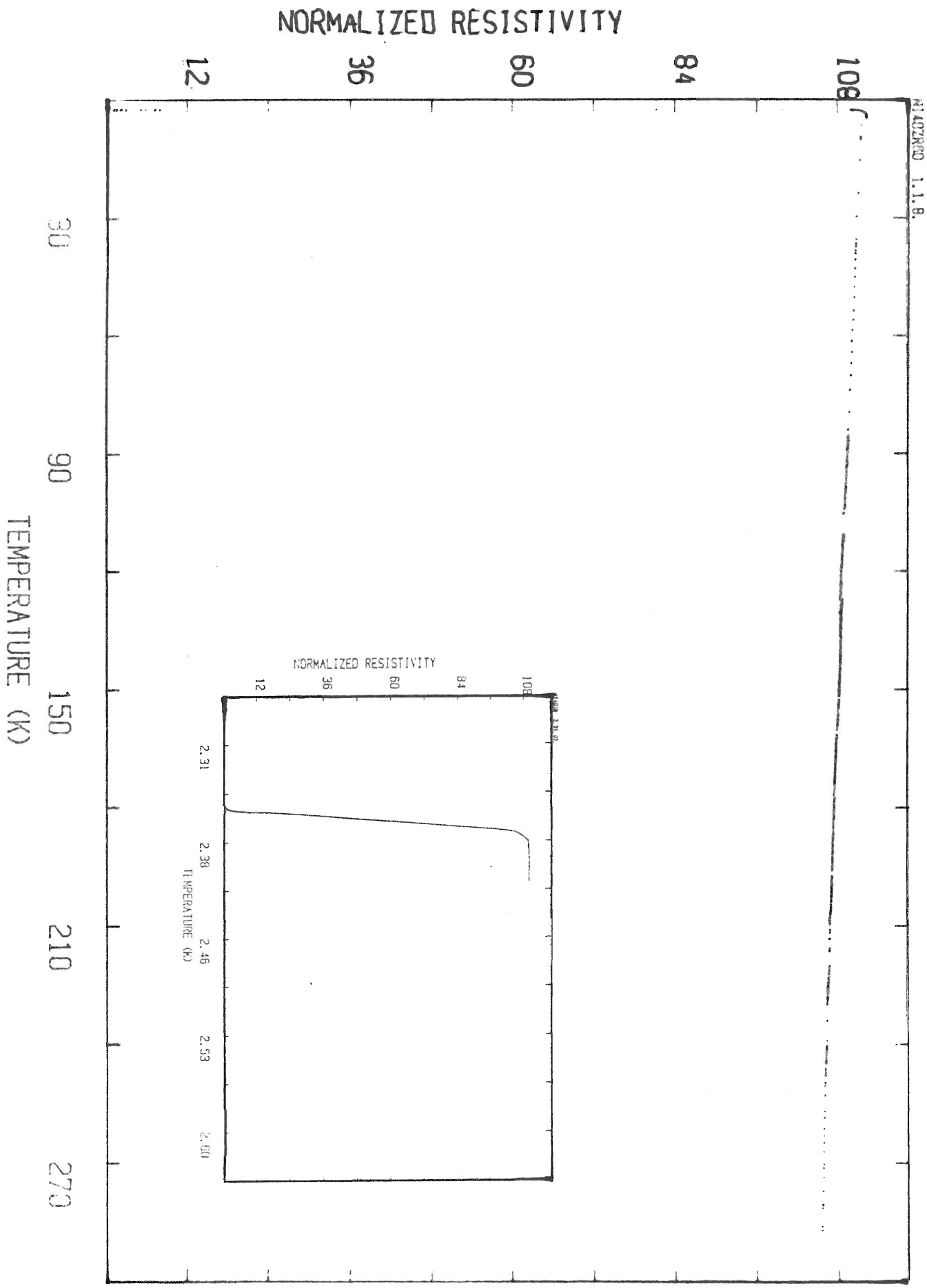
NORMALIZED RESISTIVITY
12
36
60
84
108
TEMPERATURE (K)
30
90
150
210
270
NORMALIZED RESISTIVITY
12
36
60
84
108
2.31
2.38
2.46
2.53
2.60
TEMPERATURE (K)

Figure (4-3)

Graph of resistivity of $Ni_{20}zr_{80}$ versus temperature

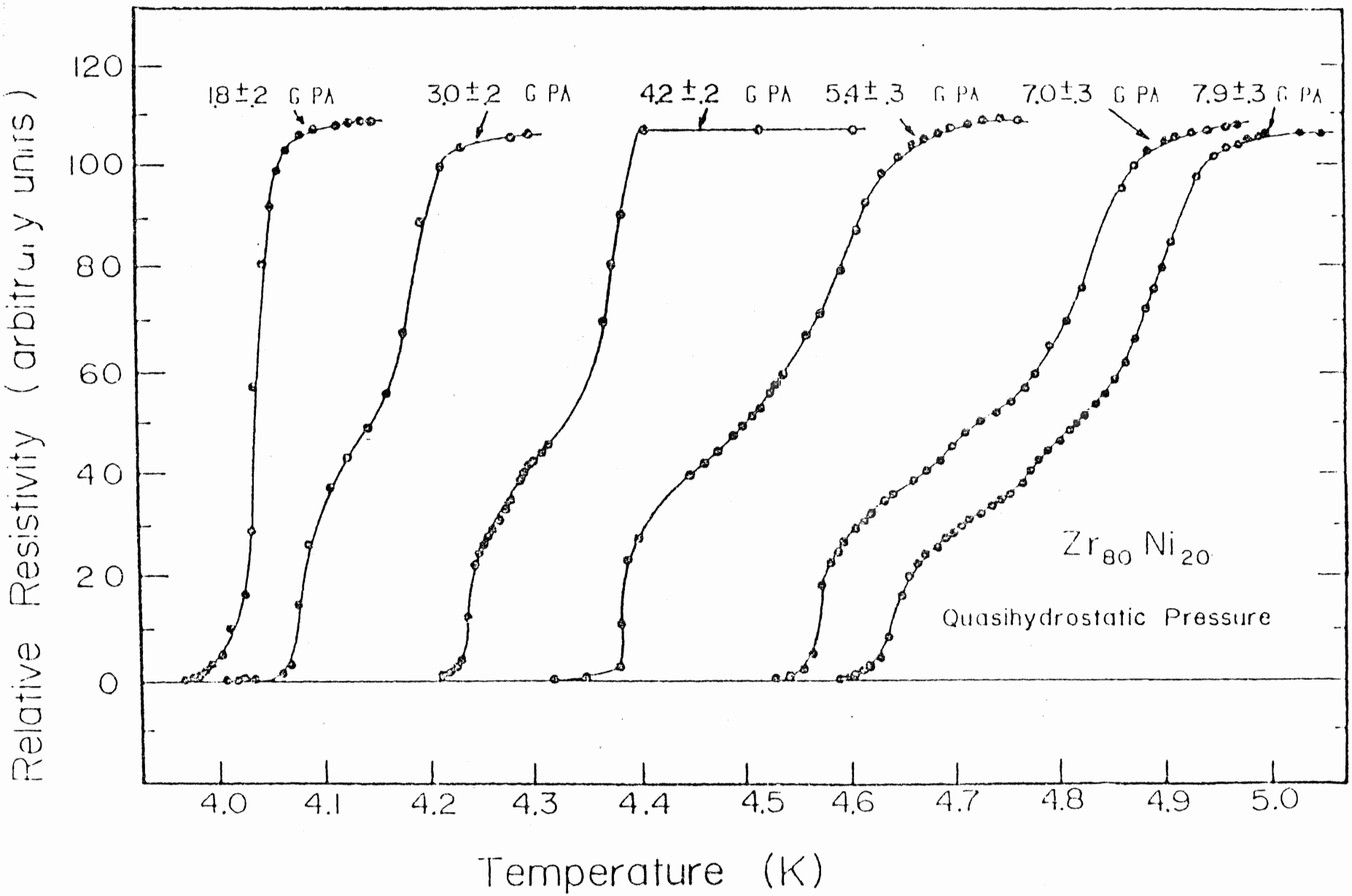
1.8±.2 G PA
3.0±.2 G PA
4.2±.2 G PA
5.4±.3 G PA
7.0±.3 G PA
7.9±.3 G PA
Zr80 Ni20
Quasihydrostatic Pressure
Relative Resistivity (arbitrary units)
120
100
80
60
40
20
0
4.0
4.1
4.2
4.3
4.4
4.5
4.6
4.7
4.8
4.9
5.0
Temperature (K)

Figure (4-4)

Graph of transition temperature of $Ni_{20}Zr_{80}$ versus pressure at low temperatures.

(● This point has been obtained from extrapolation)

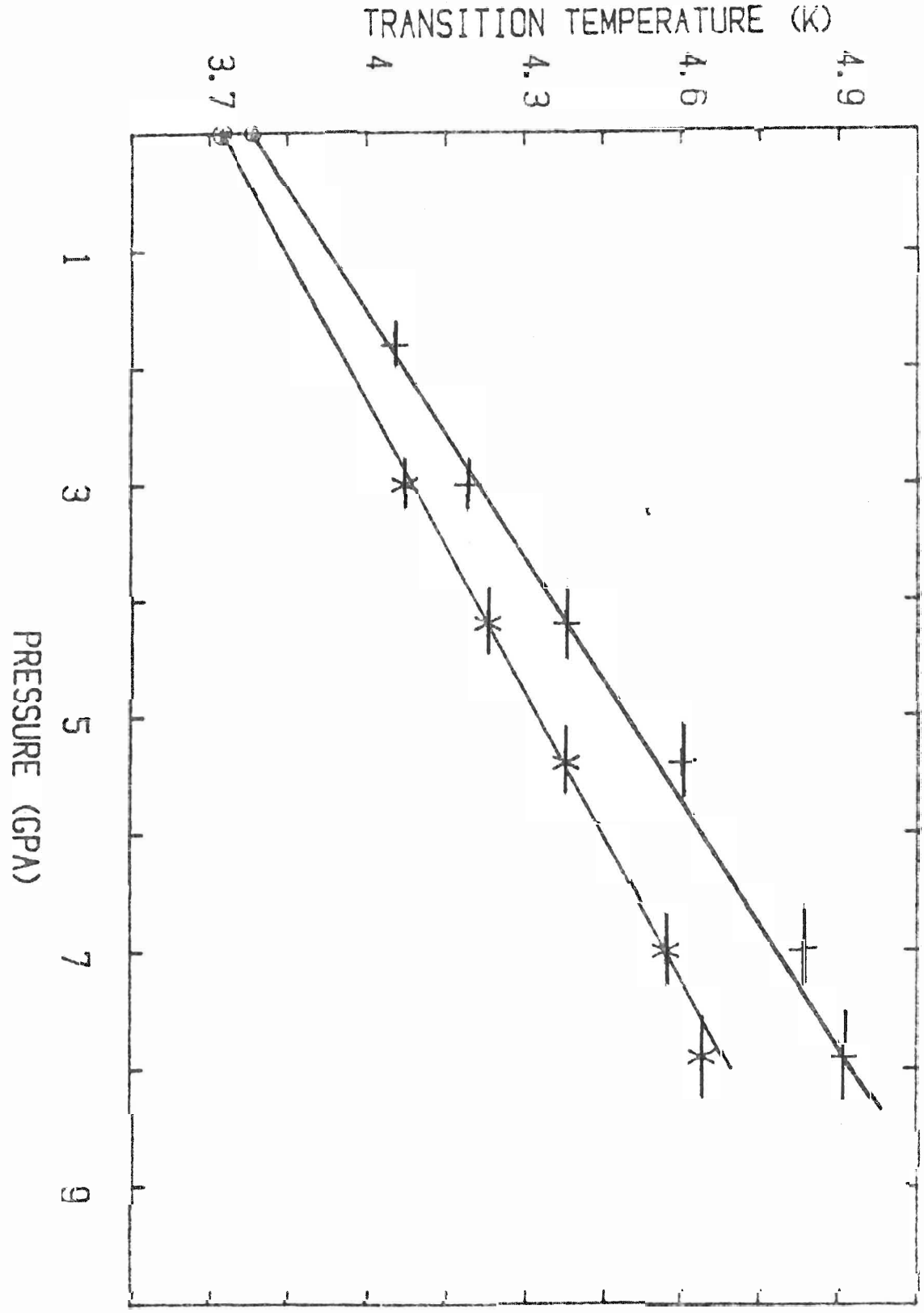
TRANSITION TEMPERATURE (K)
3.7
4
4.3
4.6
4.9
PRESSURE (GPA)
1
3
5
7
9

Figure (4-5)

Graph of transition temperature of $Ni_{29}Zr_{71}$ versus pressure at low temperatures.

(⊗ This point has been obtained from extrapolation)

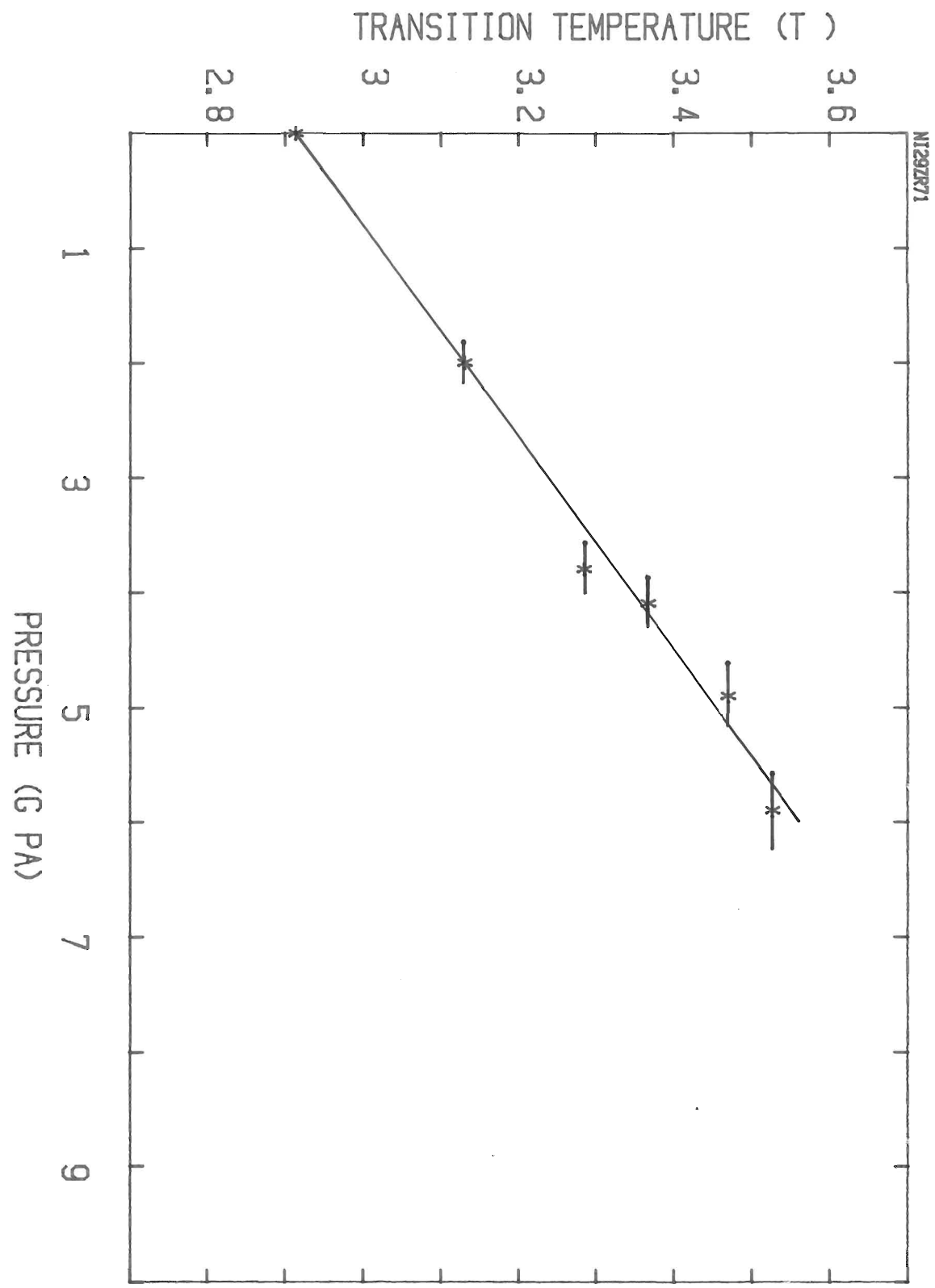
TRANSITION TEMPERATURE (T)
2.8
3
3.2
3.4
3.6
NI29ZR71
1
3
5
7
9
PRESSURE (G PA)

Figure (4-6)

Graph of transition temperature of $Ni_{36.5}Zr_{63.5}$ versus pressure at low temperatures.

(⊗ This point has been obtained from extrapolation)

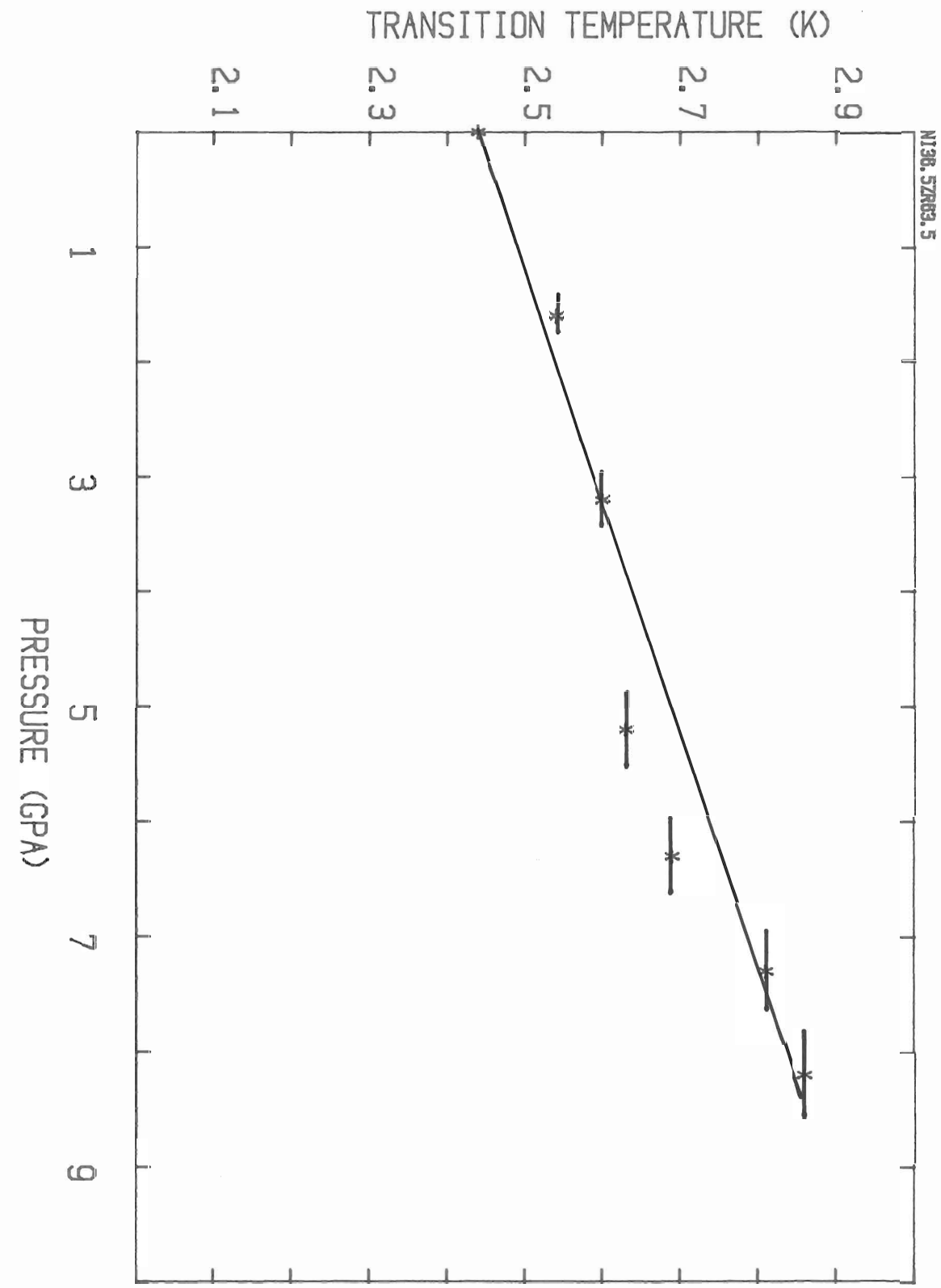
TRANSITION TEMPERATURE (K)
2.1
2.3
2.5
2.7
2.9
NI36.5ZR63.5
1
3
5
7
9
PRESSURE (GPA)

Figure (4-7)

Graph of transition temperature of $Ni_{40}Zr_{60}$ versus pressure at low temperatures.

(⊗ This point has been obtained from extrapolation)

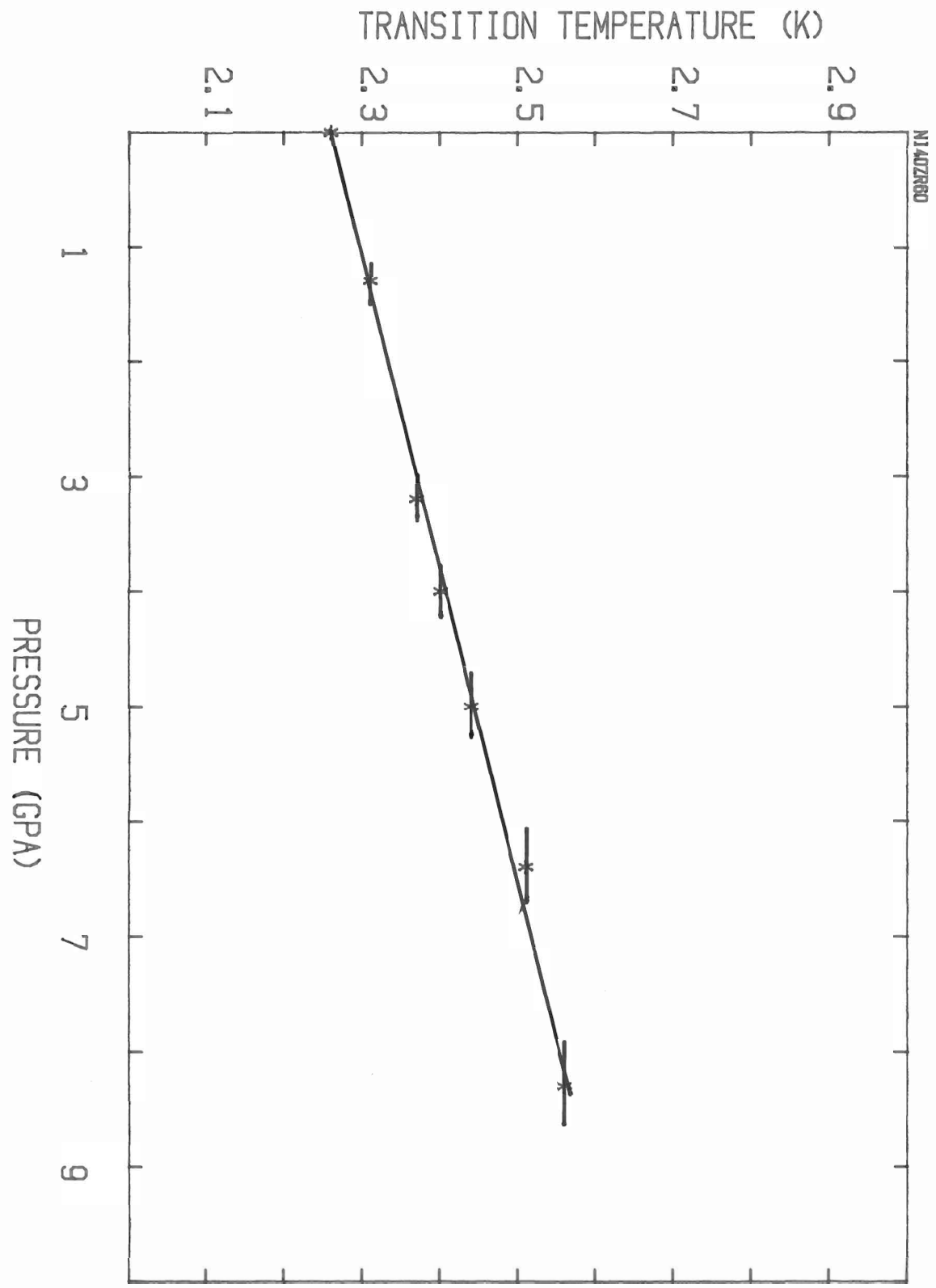
TRANSITION TEMPERATURE (K)
2.1
2.3
2.5
2.7
2.9
PRESSURE (GPA)
1
3
5
7
9
NI40ZR60

Figure (4-8)

Graph of transition temperature of $Ni_{45}Zr_{55}$ versus pressure at low temperatures.

(● This point has been obtained from extrapolation)

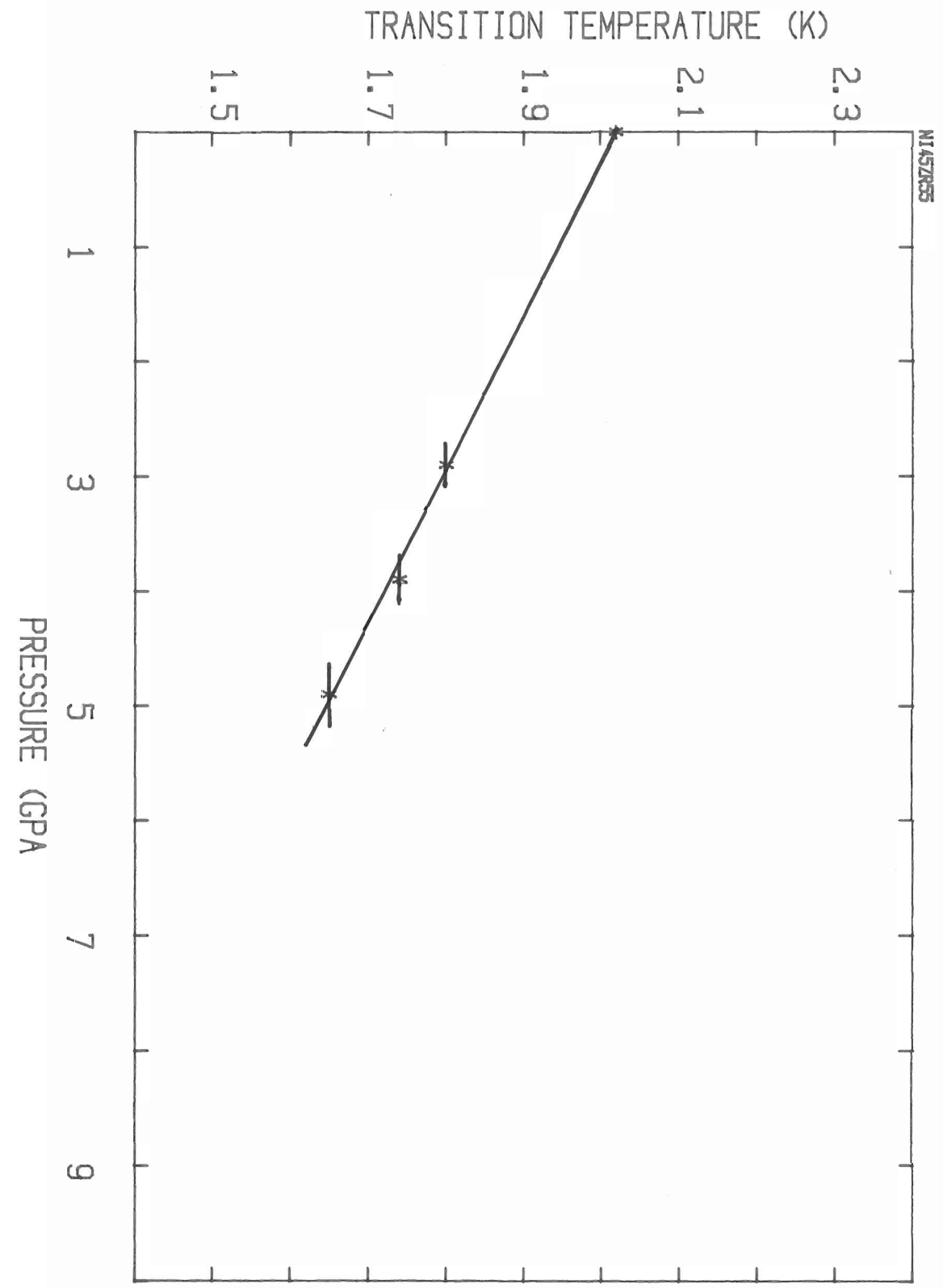
TRANSITION TEMPERATURE (K)
1.5
1.7
1.9
2.1
2.3
PRESSURE (GPA
1
3
5
7
9
NI457K65

Table 1

x (at.% Ni)	Extrapolated $T_c(0)$ K	slope $\partial T_c/\partial p$ K/G Pa*1E-2	$(\partial T_c/\partial p)1/T_c$ (1/GPa *1E-2)
20	3.77	14.8	3.924
29	2.91	10.7	3.673
33.3	2.60	8.1	3.115
36.5	2.44	4.7	1.930
40	2.26	3.72	1.648
45	2.02	-7.5	-3.708

Chapter 5

DISCUSSION

Figure (4-3) shows that $Ni_{20}Zr_{80}$ contrary to other Ni_xZr_{100-x} has (for $29=<x=<45$)a wide transition width. At pressures higher than 1.8 G Pa two transitions were clearly observed which imply the coexistence of two different phases in $Ni_{20}Zr_{80}$ amorphous alloy.

Dr. Z. Altounian has performed the X-Ray measurements on the sample piece of $Ni_{20}Zr_{80}$ pressurized to 5 G Pa. The X-Ray data showed, in addition to the usual amorphous $Ni_{20}Zr_{80}$ pattern, some lines corresponding to ω-Zr crystalline phase. The result is not surprising in view of the fact that hexagonal ω-Zr is a high pressure product of hcp α-Zr. It is the first crystallisation product if one heats the glass to 600 K. Our data suggests that ω-Zr can be formed at pressures higher than 1.8 G Pa in amorphous $Ni_{20}Zr_{80}$.

According to Olinger and Jamieson[23] the ω-Zr phase produced under pressure retains its form after pressure is released. From the

calculated d spacing and extrapolation of Olinger and Jamieson 's data to zero pressure one gets a pressure of 5 G Pa for the ω-Zr phase to form. One possibility is that with applied pressure a phase transition is taking place in the alloy. Since the pressure is applied at room temperature we should have observed a corresponding change in the resistivity of the alloy, however the change was not observed therefore this possibility is ruled out. What is probably happening here is that at high pressures, i.e. pressures greater than 1.8 G Pa, crystalline ω-Zr regions of approximate diameter 180 Å (estimated from broadening of x ray lines) are formed. As a result, the glass in the immediate vicinity of the ω-Zr crystals becomes slightly richer in Ni content and hence these regions show a lower T_c. The observed double transition corresponds to $Ni_{20}Zr_{80}$ and another alloy slightly richer in Ni. From extrapolation of $T_c(p)$ of this region to zero pressure the concentration of the alloy is estimated to be $Ni_{24}Zr_{76}$. This mechanism may explain the observed double transition in $Ni_{20}Zr_{80}$.

Figure (5-1) shows a plot of $(1/Tc)(\partial Tc/\partial p)$, the normalized change in transition temperature with pressure, versus percentage concentration of Ni present in the alloy. $(1/Tc)(\partial Tc/\partial p)$ clearly decreases

with increase in concentration of Ni and even becomes negative for Ni concentration greater than 40%.

To understand the reason for such behavior we go back to the modified McMillan equation discussed in the theory section.

The change in T_c with pressure could be attributed to the change in θ_D , λ , λ_{SF} or μ^* . We discuss each of these cases individually. If the increase in transition temperature with pressure was caused by reduction of spin fluctuation one would observe that the transition temperature is sharply increased by the pressure whether spin fluctuation is due to localized or the band model [12]. But there exists no data showing the sharp increase in transition tempeature. Increase in Ni content one also expects the spin fluctuation effects to increase[10], whereas our experiments proved otherwise. Also the negative rate of change of Tc with pressure for $Ni_{45}Zr_{55}$ also can not be explained on the basis of spin fluctuations.

Since there exists no data on the pressure dependence of the Debye temperature θ_D, we estimated the change in θ_D as a function of pressure using the compresibility results[24] and a Gruneisen parameter of about 1.5 estimated from other Zr-amorphous alloys[25]. Our estimate for the

Figure (5-1)

Graph of normalized change in transition temperature with pressure versus the atomic percentage of Ni.

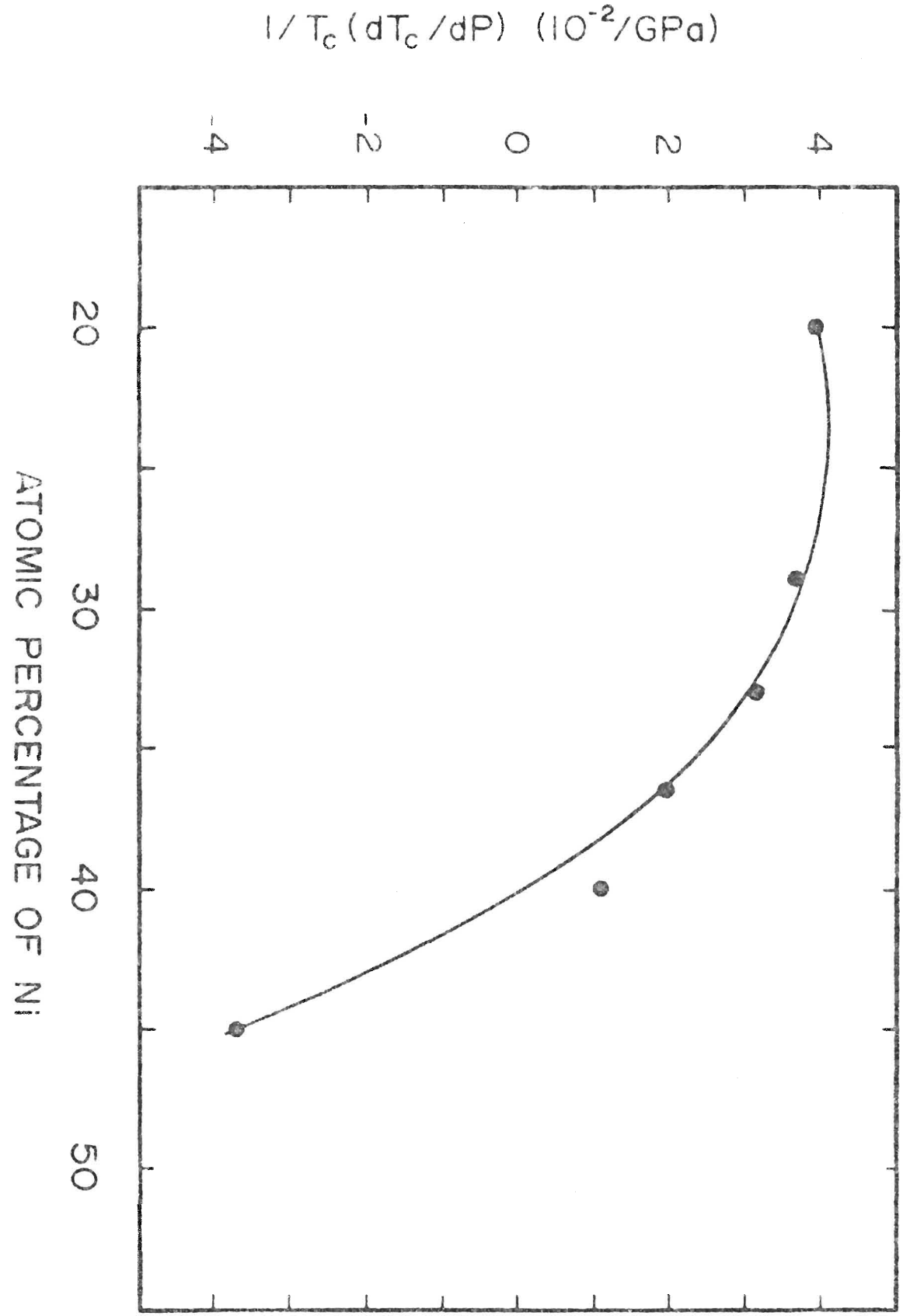
$1/T_c\,(dT_c/dP)\ (10^{-2}/GPa)$
-4
-2
0
2
4
20
30
40
50
ATOMIC PERCENTAGE OF Ni

change in Debye temperature as a function of pressure is of the order of 20% and 16% for $Ni_{20}Zr_{80}$ and $Ni_{45}Zr_{55}$, respectively. Thus, this change in Debye temperature alone cannot account for the observed 75% change in $(1/T_c)\,\partial T_c/\partial p$ from 20% Ni to 40% Ni concentration as well as a negative $(1/T_c)\partial Tc/\partial p$ for $Ni_{45}Zr_{55}$.

The Coulomb pseudopotential μ^* has been considered as constant with pressure. It has been observed that [12] the transition temperature is not sensitive to small changes in μ^*.

The variation in T_c with pressure could be due to a change in the electron phonon coupling constant which is directly proportional to electron density of states at Fermi level N(0) [12] according to

$$\lambda = N(0)\,\langle g^2\rangle\,/M\,\langle w^2\rangle$$

where $\langle g^2\rangle$ is a double average over the Fermi surface and a sum over phonon polarization indices of the square of matrix elements , M is the average ionic mass and $\langle w^2\rangle$ is the average squared phonon frequency.

Cochrane et al [1] have observed that for amorphous Ni_xZr_{100-x} alloys the Hall coefficient is positive for Ni concentration below 40 atomic percent and negative above this concentration. A similar behaviour

has been observed for thermoelectric power of this family of alloys by Altounian et al [2]. The thermoelectric power changes sign at the Ni rich end as well as observation of a strong concentration dependence of the thermoelectric power.

To account for this change in sign Cochrane et al [1] have argued that s-d hybridization and a broad Zr-4d band at the Zr rich end is responsible for the positive Hall coefficient and the narrower Ni-3d band at Ni rich end is responsible for the negative Hall coefficient.

The data of the present work agrees well with the above description by Cochrane et al [1]. The increase in pressure for Ni concentrations upto 40 percent will increase the s-d hybridization which in turn increases the density of states $N(E_f)$ and hence gives rise to a higher electron phonon coupling ϵ_p constant and consequently the T_c increases with pressure. This agrees well with our experiment. As we move to a higher concentration of Ni, the 4d band character diminishes by the addition of 3d band character of Ni and, therefore, s-d hybridization is reduced. As a result T_c changes more slowly with pressure.

In $Ni_{45}Zr_{55}$ the density of states has a 3d character. Therefore application of pressure causes the broadening of the 3d band which

reduces the density of states at the Fermi level. As a result, Tc decreases with pressure, as has been observed experimentaly in the present work.

Chapter 6

CONCLUSION

The superconducting property of Ni_xZr_{100-x} (x=20 to x=45) was studied under quasihydrostatic pressures of up to 8 G Pa.

T_c increased with pressure for concentrations of Ni upto 40%, and decreased with pressure for $Ni_{45}Zr_{55}$. The rate of change of T_c with pressure decreased with increase in concentration of Ni. These results showed that variation in T_c as a function of concentration with pressure is not caused by a change in the spin fluctuation mass enhancement factor λ_{sf}. The change in T_c as a function of pressure can be explained in terms of the character of the conduction carriers at the Fermi surface.

In addition, minute fractions of ω-Zr crystal were formed by applying pressures of greater than 1.8 G Pa to $Ni_{20}Zr_{80}$. As a result, in the immediate vicinity of these crystals the concentration of Ni becomes slightly larger, producing two phases of the amorphous alloys. Therefore it causes a double transition in the resistivity versus temperature graph.

REFERENCES

(1) Cochrane, R.W., Destry, J. and Trudeau, M. : Phys. Rev B, 27, 5977, (1983)

(2) Altounian, Z. Foiles, C.L., Muir, W.B. and Storm-Olsen, J.O. : Phys. Rev B 27, 1955 (1983)

(3) Buckle, W. and Hilsch, R. : Z. Physik, 138, 109, (1954)

(4) Elliot, S.R. : Physics of amorphous material (Printed by Long man Inc., 1983, New York)

(5) Zallen, Richard : Physics of amorphous solids (Printed by John Wiley and sons, 1983, USA)

(6) Collver, M.M., and Hammond, R.H. : Phys. Rev. Lett., 30, 92 (1973)

(7) Johnson, W.L., Poon, S.J. and Duwez, P. : Phys. Rev. B 11, 150, (1975)

(8) Rapp, O., Lindberg, B., Chen, H.S. and Rao, K.V. : J. Less Common Metals, 62, 221 (1978)

(9) Babic, E.,Ristic, R. and Miljak, M. : Solid State Communications 39, 139 (1981)

(10) Altounian, Z. and Strom-Olsen, J.O. : Phys. Rev. B 27, 4149 (1983)

(11) Batalla, E., Altounian, Z. and Strom-Olsen, J.O. : Phys. Rev. B 31, 577 (1985)

(12) Garland, J.W. and Benneman, K.H. : Superconductivity in d- and f-band metals. Douglas, D.H.(ed) A.I.P. Conf. Proc. No. 4. New York: American Inst. of Physics, 103 (1972)

(13) Onnes, H.K. : Comm.Phys. Lab. Univ. Leiden Nos. 119,120 ,122 (1911)

(14) Kittel, C. : Introduction to solid state physics (John Wiley and Sons, Inc, 1976), pp 355-398

(15) Bardeen, J., Cooper, L.N. and Schrieffer, J.R. : Phys. Rev., 108 , 1175 (1957)

(16) McMillan, W.L. : Phys. Rev. ,167 , 331 (1968)

(17) Allen, P.B. and Mitrovic, B. : Solid state Physics edited by Ehrenreich, H., Seitz, F., Turnbull, D., (Academic, New york, 1982), Vol. 37, PP 1-92

(18) Moriya, Spin Fluctuations in Itinerant Electron magnetism. (Springer series in Solid State Sciences; Vol. 56) (Springer-Verlag, Berlin, 1985)

(19) Guntherodth, H.J. : Spring meeting of the solid state division of the German Physical Society, Munster, Germany, 7-12 March 1977 (Braunschweig, Germany : Friedr. Vieweg and Sohn 1977, p. 25)

(20) Altounian, Z, Gua-Hua, Tu and Strom-Olsen, J.O. : J. Appl. Phys. 54 (16), 3111 (1983)

(21) Buschow, K. H. J., Verbeek, B.H. and Dirks, A. G. : J. Phys. D, 14, 1087 (1982)

(22) Eichler, A. and Witting J. : Z. Angew. Physica 25, 319 (1968)

(23) Olinger, B. and Jamison, J. C. : High temperature high pressure, vol. 5, 123 (1973)

(24) Cochrane, R. W., Destry, J. Amrani, El, Altounian, Z. and Strom-Olsen, J. O. : Rapidly quenched metals 1083 (1985)

(25) Fritsch, G. Willer, J., Wildermuth, A. and Luscher, G. : Physics of solids under high pressure 239 (1981)